Microscopy Reveals: Impact of Lithium Salts on Elementary Steps Predicts Organozinc Reagent Synthesis and Structure

Kristof Jess, Kazuhiro Kitagawa, Tristen K. S. Tagawa, and Suzanne A. Blum*

Department of Chemistry, University of California, Irvine, CA 92697-2025, USA

Supporting Information Placeholder

ABSTRACT: Lithium chloride is known to promote the direct insertion of metallic zinc powder into organohalides in the practical synthesis of organozinc reagents, but the reason for its special ability is poorly understood. Pioneering a combined approach of single-metal-particle fluorescence microscopy with ^{1}H NMR spectroscopy, we herein show that the effectiveness of different lithium salts towards solubilizing intermediates on the surface of zinc metal establishes a previously unknown reactivity correlation that predicts the propensity of that salt to promote macroscale reagent synthesis and also predicts the solution structure of the ultimate organozinc reagent. A salt-free pathway is also identified. These observations of an organometallic surface intermediate, its elementary-step reactivity, and the impact of various synthetic conditions (salt, salt-free, temperature, stirring, time) on its persistence, are uniquely available from the sensitivity and spatial localization ability of the microscopy technique. These studies unify previously disparate observations under a single unified mechanistic framework. This framework enables the rational prediction of salt effects on multiple steps in organozinc reagent synthesis and reactivity. This is an early example of single-particle microscopy characterization of elementary steps providing predictive power in reaction development by gaining a sensitive and selective spectral handle on an important intermediate, highlighting the role of this next generation of analytical tools in the development of synthetic chemistry.

Introduction. The finding by Knochel in 2006 that LiCl substantially enhanced the rate of the direct insertion reaction of organohalides to zinc metal[1] led to a series of discoveries for the practical preparation of organometallic reagents from metal powders. The resulting reagents are useful, for example, as transmetallation partners in Negishi cross-coupling reactions.[2] Whereas only organomagnesium (Grignard) reagents used to be widely accessible by direct insertion of metals into organohalides,[3,4] the organometallic toolbox was expanded to zinc,[1] indium,[5–7] manganese,[8] and aluminum[9] through the addition of lithium chloride, sometimes in combination with transition metal additives.[10] Yet the mechanistic role of LiCl and the impact of the presence of additives on the structure of the resulting organozinc reagents remains poorly understood, limiting the expansion of salt effects that promote oxidative addition to other metals. The nature of the organometallic reagents that form from these reactions is of the utmost importance to understand, as the presence of salts left over is known to alter reactivity, often favorably.[11,12] This observation raises the possibility that other lithium salts[13] would also be valuable synthetically, though to our knowledge no others have been reported with a single exception of LiBr.[12] The reason for the limited understanding is the inability of traditional analytical techniques to probe reactions and small quantities of intermediates at the surface of metals under reaction conditions.[14]

Pioneering a combined single-metal-particle microscopy approach that is sensitive enough to overcome these analytical limitations with an ^{1}H NMR spectroscopy approach,[15] we here discover that the impact of different salts on the solubilization of zinc surface intermediates predicts both the rate acceleration in macroscale synthesis and the solution structure of the ultimate organozinc reagent (Figure 1). The fluorescence microscopy experiments provide information about behavior of intermediates in elementary steps, whereas the NMR spectroscopy experiments provide information about overall reaction rate and product structure. The resulting new synthetic knowledge provides a robust theoretical framework that unifies the understanding of previously disparate multiple steps of the salt-mediated syntheses of organozinc reagents, making the effect of lithium salts on multiple steps predictable under one model.

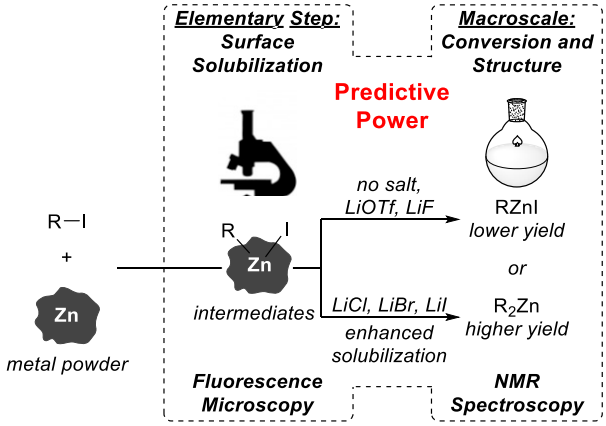

Figure 1. Synergistic approach.

Results and Discussion.

Single-Particle Fluorescence Microscopy Study. We recently showed that fluorescence microscopy with sensitivity as high as to the single-molecule level[15–21] can characterize the presence and reactivity of previously unknown oxidative addition intermediates on the surface of zinc metal.[22] In the experimental design, imaging agent **1** is employed as a probe for oxidative addition surface reactivity. It consists of a BODIPY (boron dipyrromethene) unit that acts as a spectator fluorophore, an oxidative addition reactive carbon–iodide bond, and a

butyl linker separating the BODIPY unit electronically and sterically from the oxidative addition site (Figure 2, inset). Imaging agent **1** in solution is not imaged because it is diffusing rapidly. Oxidative addition to the zinc surface builds up surface intermediates, depicted as **2**. Previous control experiments[16,22] are consistent with assignment of **2** as the product of oxidative addition/direct insertion of the surface zinc atoms into the C–I bonds of **1**, upon which the imaging agent becomes stationary and is imaged as bright green "hot spots" on the surface of the previously dark zinc particles (Figure 2, top schematic). As we showed previously, intermediate **2** is persistent in the absence of a salt, but is solubilized rapidly upon addition of LiCl, leaving behind dark zinc particles.[22]

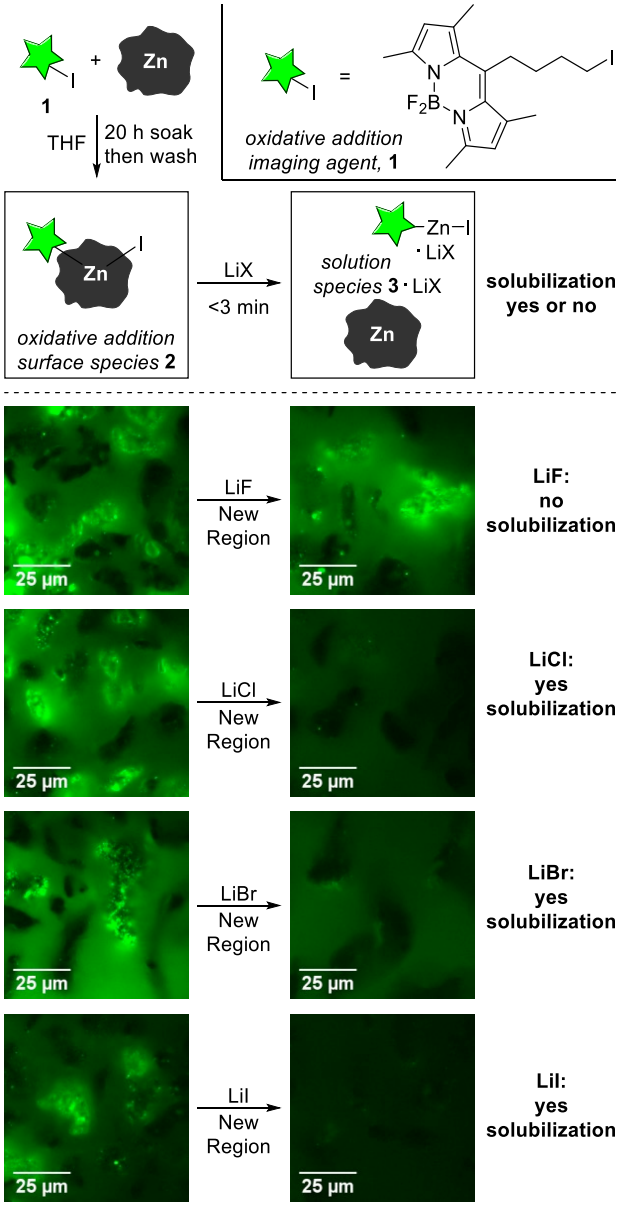

Figure 2. Top: Schematic of the fluorescence microscopy experiments. Inset: Imaging agent for oxidative addition. Below: Experimental fluorescence microscopy images show the effect of addition of solid salts to different aliquots of zinc samples of **2** in THF. All images are displayed at identical brightness/contrast settings to allow direct comparison. An explanation of new regions is described in Figure S1.

In the present study, we examined microscopy images of zinc particles with bright green "hot spots" of **2** before and after addition of different lithium salts LiX (X = F, Cl, Br, I; t = 90–150 s after addition; Figure 2). In this way, it was possible to analytically study isolated single elementary reaction steps. Specifically, the impact of different lithium salts on the solubilization of oxidative addition surface intermediates could be independently determined. Images from LiF addition showed little to no difference in fluorescence intensities or quantities of the "hot spots" before and after, meaning that LiF addition did not noticeably solubilize intermediate **2** and remove it from the zinc surface (Figure 2). This observation with LiF is the same as with LiOTf from our previous studies.[22] In contrast, directly after addition of LiCl, LiBr, or LiI the green fluorescent spots disappeared or became significantly dimmer across the entire sample (representative images, Figure 2). Although it is impossible to find and study the exact same particles before and after salt addition, the effect caused by salt addition is fully consistent throughout the sample (see Supporting Information for movies of whole sample). Based on our previous studies,[16,22] we interpret these findings as LiF and LiOTf being inefficient at solubilizing organozinc intermediate **2**, whereas LiCl, LiBr, and LiI are efficient at solubilizing **2** to generate solution species **3**·LiX (Figure 2). Control experiments ruled out quenching of fluorescence by lithium salts or adventitious water as the causes of these results (see Supporting Information). These microscopy results are significant because they identify important elementary steps in the macroscale generation of organozinc reagents directly from zinc metal powder and because they predict that LiBr[12] and LiI are promising candidates as additives for macroscale synthesis, whereas LiF and LiOTf are not.

The spatial and reactivity distribution of intermediate **2** in Figure 2 reflects the range of reactivity inherent to the synthetic system: The same supplier and mesh of zinc particles were used as in the reported synthetic procedure by Knochel,[1] allowing detection of the heterogeneity of reactivity germane to the "real" synthetic reaction. These particles reacted differently, and even different locations on the same particle were found to vary significantly in their reactivity, as detected as a range of brightness and distribution of fluorescent intermediate **2**. This distribution is uniquely revealed by the sensitivity and spatial resolution of the microscopy approach and is obscured by a purely NMR spectroscopy approach that does not have sensitivity sufficient for detection of **2** nor spatial/localization characterization ability.

We next investigated if there might be an alternative, salt-free pathway accessible for solubilization of otherwise-persistent surface intermediate **2** (Figure 3). For this experiment, a single sample of **2** was divided into portions for comparison, and treated with different salt-free conditions that would mimic those present in a bulk synthetic reaction:

A first portion was soaked for 2 h in standing THF. This sample showed little change and established continued persistence of **2**. A second portion was stirred for 2 h in THF. This sample showed a middle extent of solubilization of **2**, visible as a reduction in the brightness and extent of coverage of bright green "hot spots" and more completely dark particles with no detectible **2**. Smaller particles of zinc powder were generated through this stirring process, which were distinctly observable post-stirring (see SI for movie and details). The generation of these smaller particles suggested that stirring may assist solubilization of **2** by breaking apart larger zinc particles into smaller particles with higher surface area, or by removing the surface layer of zinc by interparticle friction (e.g., analogous to "sandblasting"). A third portion

was soaked for 2 h with heating at 100 °C. This sample exhibited substantial solubilization of **2**, as evidenced by widespread reduction in the number and brightness of the green "hot spots" and widespread presence of fully dark zinc particles without detectable **2**. The images in Figure 3 are representative single frames from movies that examined the entire samples (see SI). Thus, a continuum of persistence−solubilization occurred in salt-free systems, depending on sample conditions analogous to those that might be present under bulk-scale synthetic conditions.

Together, these data are consistent with the accessibility of a higher-barrier solubilization of intermediate **2** under salt-free synthetic conditions or in the presence of an ineffective salt. This pathway was notably slower than that assisted by LiCl, LiBr, and LiI (for comparison, <3 min, ambient temperature, Figure 2). Therefore, a slower salt-free pathway should also be accessible in the synthetic reaction for formation of alkylzinc reagents with sufficient heating or stirring.

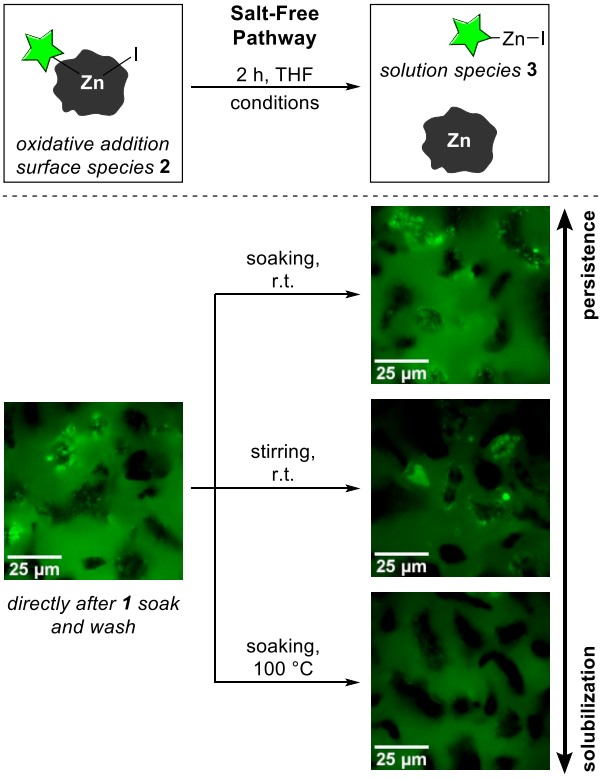

Figure 3. Top: Schematic of the fluorescence microscopy experiments. Below: Fluorescence microscopy images showing higher barrier salt-free solubilization. All images are displayed at identical brightness/contrast settings to allow direct comparison.

These observations of organometallic intermediate **2**, its elementary-step reactivity, and the impact of synthetic conditions (salt, salt-free, temperature, stirring, time) on its persistence, are uniquely available from the sensitivity and spatial localization ability of the microscopy technique. This mechanistic information is fully obscured by traditional analytical techniques such as NMR spectroscopy, through which only the starting alkyl iodide and product organozinc are observable, but not intermediate **2** nor its pathways, nor its apparent rate-limiting behavior in the overall transformation. Instead, fluorescence microscopy gains a sensitive and selective spectral handle on an important intermediate that NMR spectroscopy could not capture. These microscopy observations predicted bulk-scale synthetic outcomes, as will next be described.

^{1}H NMR Spectroscopy Study. To investigate if the trend observed by fluorescence microscopy predicted which salts would be effective in accelerating the rate of synthesis of organozinc reagents, we studied the conversion of (2-iodoethyl)benzene (**4**) to its corresponding organozinc species **5** by ^{1}H NMR spectroscopy (Table 1). The deliberately ambiguous notation used by Knochel, "**5**·LiX" in Table 1, avoids implying a structure.[1,23] Substrate **4** was reacted with 1.4 equiv of zinc and 1 equiv of LiX; a control experiment without any salt additive was also conducted. In these experiments, it is evident that there are two sets of conditions: experiments with LiF, LiOTf, or without any salt gave lower conversions (56–62%: Set 1), whereas experiments with LiCl, LiBr, and LiI gave full conversion (Set 2). These outcomes on the macroscale correlate with the reactivity trend observed by fluorescence microscopy in that they sort the salts into the *same* two sets. This observation provides compelling support for the conclusion that the ability of a salt to solubilize surface intermediates is the mechanistic cause of the rate enhancement observed in the macroscale synthetic reaction.

Table 1. Salt Effect Observed on Intermediates by Fluorescence Microscopy Predicts Macroscale Synthesis Effects.

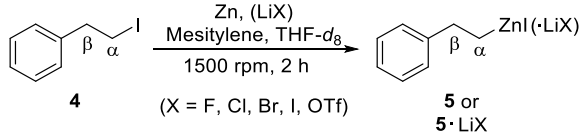

Salt	NMR Conversion [%]	Solubilization of **2** in Elementary Step[a]	
No salt	57	--	
LiOTf	62	no	***Set 1***
LiF	56	no	
LiCl	99	yes	
LiBr	99	yes	***Set 2***
LiI	>99	yes	

[a] See Figure 2. LiOTF data from previous experiments.[22]

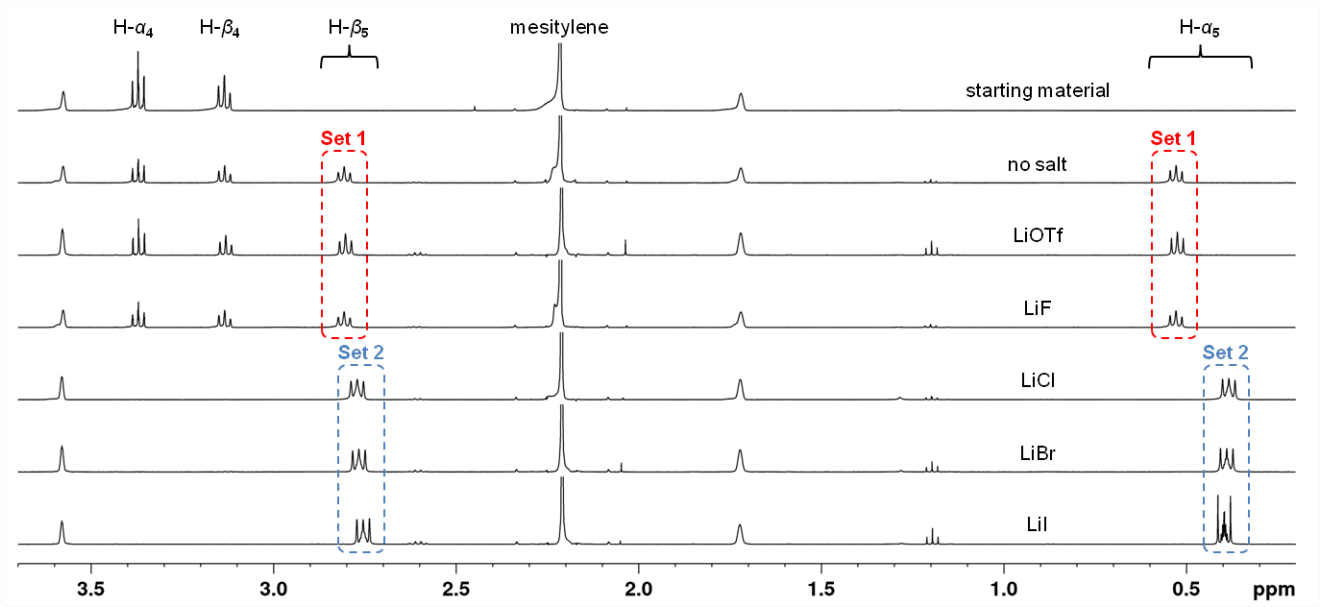

Figure 4. ^{1}H NMR spectra (THF-d_8, 500 MHz, 300 K) for the reaction of (2-iodoethyl)benzene (**4**) with zinc as described in Table 1. Letter α denotes signals for CH_2–I in **4** or CH_2–Zn in products **5** or **5**·LiX and letter β denotes signals for CH_2–Ph.

Next, a closer examination of the ^{1}H NMR spectroscopy data revealed that the two sets of salts identified in the microscopy experiments generated two sets of structurally different organozinc reagents in solution (Figure 4).

Set 1. Organozinc compounds formed in the presence of LiF, LiOTf, or no salt, exhibit α methylene protons further downfield, at 0.53 ppm, independent of the presence or nature of lithium salts in this set. This result indicates that the identical organozinc product is formed in all three cases, assigned as monomeric RZnI[24–26].

Set 2. Organozinc compounds formed in the presence of LiCl, LiBr, and LiI exhibit α methylene protons at 0.38−0.39 ppm, almost independent of the nature of the lithium salts within this set. This independence suggests that these samples likely contain the same major equilibrium structure, but a different structure than that formed in Set 1. We previously detected $[RZnX_2]^-$ by negative ionization ESI-MS in reactions of **1** with Zn in the presence of LiCl,[16] similar to the types of complexes observed by Koszinowski.[27,28] In previous studies by Organ using ^{1}H NMR spectroscopy and ESI-MS, it was suggested that for the LiBr assisted organozinc formation in THF, a plausible product is the neutral diorganozinc compound R_2Zn (from Schlenk equilibrium with mass balance of $Li[ZnBr_3]$, eq 1).[29] In accordance, our own ^{1}H NMR spectral data presents compelling evidence that the same organozinc structure is formed regardless of the nature of X in this set; thus, R_2Zn appears to be the main organozinc equilibrium structure in all cases within salt Set 2.

$$\underset{\substack{\textit{favored side}\\ \textit{no LiX or OTf, F}}}{2\ RZnX + LiX} \underset{\text{THF}}{\overset{\textit{Schlenk equilibrium}}{\rightleftharpoons}} \underset{\substack{\textit{favored side}\\ \textit{Cl, Br, I}}}{R_2Zn + Li[ZnX_3]} \quad (1)$$

Distinct coupling patterns further confirm the existence of two different sets of solution structures for these organozinc reagents. Figure 5 shows expansions of the α proton regions. The signals from organozinc compounds derived from LiCl, LiBr, and LiI are prominent second-order AA'XX' coupling patterns, providing strong evidence for a shared conformational[30] structural feature.

In contrast, the signals arising from the organozinc compound generated in the presence of LiF, LiOTf, or no salt did not display this pattern. These signals likely all arise from the identical compound, RZnI[24]. ^{7}Li NMR spectroscopy data is further consistent with this assignment (see Supporting Information for details).

These ^{1}H NMR spectroscopy data provide compelling evidence that the two classes of lithium salts, identified first by microscopy to produce *reactivity* differences on solubilization of intermediates from the zinc surface, produce two different macroscale rate classes, and two different *structural* classes of organozinc reagents in solution. This correlation was previously unknown, and thus provides a new conclusion about reactivity.

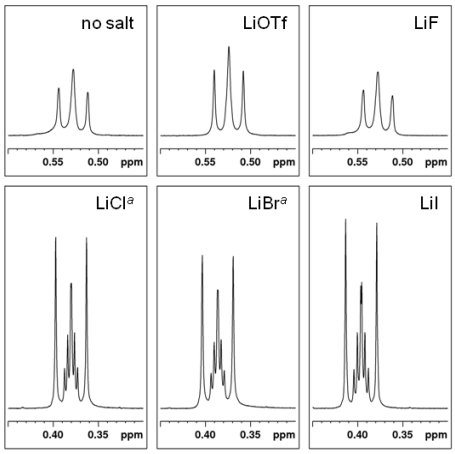

Figure 5. ^{1}H NMR spectroscopy expansion of the methylene groups H-α on organozinc **5** (·LiX). [a] In the case of LiCl and LiBr

the expansion from Figure 4 showed artefacts from misadjusted shim, therefore the corresponding expansions from a different set of experiments are shown here for clarity.

Unified Theoretical and Predictive Model. The propensity of the anion X to coordinate to zinc to form a zincate is the crucial difference for solubilization of the surface intermediate, which causes accelerated organozinc reagent formation. The same propensity dictates the final solution structure of the reagent formed after equilibrium is established, with a strong binding X shifting the Schlenk equilibrium and a weak binding X not shifting the Schlenk equilibrium (eq 1). Figure 6 shows a depiction of intermediates/transition states, involving the critical coordination of the second halide of Cl, Br, and I to zinc as part of the solubilization step (Set 2). This zincate is apparently more soluble than the neutral organozinc complex in THF, leading to its faster dissolution from the surface. Plausibly this enhanced solubility arises from the known coordination of lithium cations by THF, resulting in a nonequilibrium complex of $(THF)_nLi[RZnX_2]$, which is responsible for the release of the organozinc species from the surface. This complex is then available to equilibrate in solution to $R_2Zn + Li[ZnX_3]$.

For the cases with LiF, LiOTf, and no salt (Set 1), another mechanism of solubilization occurs, which does not involve LiX. This solubilization pathway is evident in Figure 3. In the case of LiF, its lower solubility in THF (0.1 mM at 24 °C)[31] indicates that strong LiF bonds plausibly disfavour formation of Li[RZnIF]. The weakly coordinating nature of triflate plausibly reduces its propensity for binding to zinc. Thus, in the absence of sufficient propensity of X to coordinate, a higher-barrier salt-free solubilization pathway is predominant, producing solution-phase RZnI.

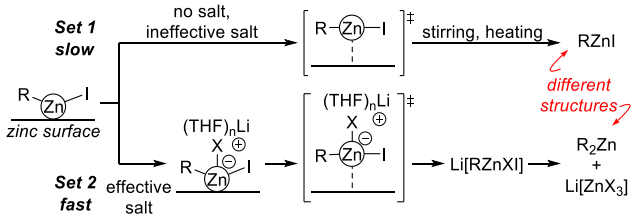

Figure 6. Unifying theoretical and predictive model.

Conclusion. Combined ^1H NMR spectroscopy and fluorescence microscopy studies showed that the solubilization behavior of intermediate **2**, observed by microscopy with different lithium salts, correlated with reaction acceleration in the bulk synthesis of **5**. This correlation enabled *synthetic prediction* of which lithium salts would or would not accelerate bulk reagent synthesis of **5**, including those which had not yet been reported, on the basis solely of the salt's effect on solubilization of intermediate **2** observed by microscopy. This is an early example of single-particle fluorescence microscopy applied to answering mechanistic questions in organic/organometallic chemistry through imaging intermediates that do not build up to quantities needed for observation by traditional analytical tools. The experiments here firmly established a connection between microscopic behavior of intermediates and macroscopic synthesis effects, opening additional avenues for this type of multidisciplinary research in the future. This connection shows the power of the combined analytical techniques to answer previously intractable mechanistic questions in synthesis. We anticipate that this method could be applied to a range of other oxidative addition and related reactions. From a synthetic standpoint, these conclusions enable rational development of organometallic reagents directly from metal powders with salt additives, a broadly desirable reaction class in synthetic chemistry that has been previously limited by its empirical development.

ASSOCIATED CONTENT

Supporting Information

The Supporting Information is available free of charge on the ACS Publications website.
Experimental details, replicate microscopy data, movies, $^1H/^7Li$ NMR data, details of control experiments (PDF, AVI).

AUTHOR INFORMATION

Corresponding Author

*blums@uci.edu

Notes

The authors declare no competing financial interests.

ACKNOWLEDGMENT

We thank the National Science Foundation (CHE-1464959) and the University of California, Irvine (UCI), for funding. K. J. thanks the German Research Foundation (DFG) for a fellowship (JE 886/1-1) and K. K. thanks the Japan Society for the Promotion of Science for a fellowship (JP15J03538).

REFERENCES

(1) Krasovskiy, A.; Malakhov, V.; Gavryushin, A.; Knochel, P. Efficient Synthesis of Functionalized Organozinc Compounds by the Direct Insertion of Zinc into Organic Iodides and Bromides. *Angew. Chem. Int. Ed.* **2006**, *45*, 6040–6044.

(2) Negishi, E. Palladium- or Nickel-Catalyzed Cross Coupling. A New Selective Method for Carbon-Carbon Bond Formation. *Acc. Chem. Res.* **1982**, *15*, 340–348.

(3) Grignard, M. V. Sur Quelques Nouvelles Combinaisons Organométalliques Du Magnèsium et Leur Application à Des Synthèses d'alcools et d'hydrocarbures. *C. R. Hebd. Seances Acad. Sci.* **1900**, *130*, 1322–1324.

(4) *Grignard Reagents*; Richey, H. G., Ed.; Wiley: Chichester, 2000.

(5) Chen, Y.-H.; Knochel, P. Preparation of Aryl and Heteroaryl Indium(III) Reagents by the Direct Insertion of Indium in the Presence of LiCl. *Angew. Chem. Int. Ed.* **2008**, *47*, 7648–7651.

(6) Papoian, V.; Minehan, T. Palladium-Catalyzed Reactions of Arylindium Reagents Prepared Directly from Aryl Iodides and Indium Metal. *J. Org. Chem.* **2008**, *73*, 7376–7379.

(7) Adak, L.; Yoshikai, N. Cobalt-Catalyzed Preparation of Arylindium Reagents from Aryl and Heteroaryl Bromides. *J. Org. Chem.* **2011**, *76*, 7563–7568.

(8) Peng, Z.; Knochel, P. Preparation of Functionalized Organomanganese(II) Reagents by Direct Insertion of Manganese to Aromatic and Benzylic Halides. *Org. Lett.* **2011**, *13*, 3198–3201.

(9) Blümke, T.; Chen, Y.-H.; Peng, Z.; Knochel, P. Preparation of Functionalized Organoaluminiums by Direct Insertion of Aluminium to Unsaturated Halides. *Nat. Chem.* **2010**, *2*, 313–318.

(10) Dagousset, G.; François, C.; León, T.; Blanc, R.; Sansiaume-Dagousset, E.; Knochel, P. Preparation of Functionalized Lithium, Magnesium, Aluminum, Zinc, Manganese-, and Indium Organometallics from Functionalized Organic Halides. *Synthesis* **2014**, *46*, 3133–3171.

(11) Ochiai, H.; Jang, M.; Hirano, K.; Yorimitsu, H.; Oshima, K. Nickel-Catalyzed Carboxylation of Organozinc Reagents with CO_2. *Org. Lett.* **2008**, *10*, 2681–2683.

(12) Achonduh, G. T.; Hadei, N.; Valente, C.; Avola, S.; O'Brien, C. J.; Organ, M. G. On the Role of Additives in Alkyl-Alkyl Negishi Cross-Couplings. *Chem. Commun.* **2010**, *46*, 4109–4111.

(13) Knochel, P.; Gavryushin, A.; Malakhov, V.; Krasovskiy, A. Verfahren Zur Synthese von Organoelementverbindungen. DE102006015378, 2007.

(14) MacQuarrie, S.; Horton, J. H.; Barnes, J.; McEleney, K.; Loock, H.-P.; Crudden, C. M. Visual Observation of Redistribution and

Dissolution of Palladium during the Suzuki–Miyaura Reaction. *Angew. Chem. Int. Ed.* **2008**, *47*, 3279–3282.

(15) Ng, J. D.; Upadhyay, S. P.; Marquard, A. N.; Lupo, K. M.; Hinton, D. A.; Padilla, N. A.; Bates, D. M.; Goldsmith, R. H. Single-Molecule Investigation of Initiation Dynamics of an Organometallic Catalyst. *J. Am. Chem. Soc.* **2016**, *138*, 3876–3883.

(16) Feng, C.; Easter, Q. T.; Blum, S. A. Structure-Reactivity Studies, Characterization, and Transformation of Intermediates by Lithium Chloride in the Direct Insertion of Alkyl and Aryl Iodides to Metallic Zinc Powder. *Organometallics* **2017**, *36*, 2389–2396.

(17) Roeffaers, M. B. J.; Sels, B. F.; Uji-i, H.; De Schryver, F. C.; Jacobs, P. A.; De Vos, D. E.; Hofkens, J. Spatially Resolved Observation of Crystal-Face-Dependent Catalysis by Single Turnover Counting. *Nature* **2006**, *439*, 572–575.

(18) Esfandiari, N. M.; Wang, Y.; Bass, J. Y.; Cornell, T. P.; Otte, D. A. L.; Cheng, M. H.; Hemminger, J. C.; McIntire, T. M.; Mandelshtam, V. A.; Blum, S. A. Single-Molecule Imaging of Platinum Ligand Exchange Reaction Reveals Reactivity Distribution. *J. Am. Chem. Soc.* **2010**, *132*, 15167–15169.

(19) Cordes, T.; Blum, S. A. Opportunities and Challenges in Single-Molecule and Single-Particle Fluorescence Microscopy for Mechanistic Studies of Chemical Reactions. *Nat. Chem.* **2013**, *5*, 993–999.

(20) Ristanović, Z.; Kubarev, A. V; Hofkens, J.; Roeffaers, M. B. J.; Weckhuysen, B. M. Single Molecule Nanospectroscopy Visualizes Proton-Transfer Processes within a Zeolite Crystal. *J. Am. Chem. Soc.* **2016**, *138*, 13586–13596.

(21) Kubarev, A. V.; Janssen, K. P. F.; Roeffaers, M. B. J. Noninvasive Nanoscopy Uncovers the Impact of the Hierarchical Porous Structure on the Catalytic Activity of Single Dealuminated Mordenite Crystals. *ChemCatChem* **2015**, *7*, 3646–3650.

(22) Feng, C.; Cunningham, D. W.; Easter, Q. T.; Blum, S. A. Role of LiCl in Generating Soluble Organozinc Reagents. *J. Am. Chem. Soc.* **2016**, *138*, 11156–11159.

(23) Koszinowski, K.; Böhrer, P. Formation of Organozincate Anions in LiCl-Mediated Zinc Insertion Reactions. *Organometallics* **2009**, *28*, 771–779.

(24) Boersma, J.; Noltes, J. G. Properties of Unsolvated Organozinc Halides. *Tetrahedron Lett.* **1966**, *7*, 1521–1525.

(25) Evans, D. F.; Fazakerley, G. V. Proton Resonance Studies of the Schlenk Equilibria for Methyl- and Ethyl-Zinc Iodide in Tetrahydrofuran. *J. Chem. Soc. A Inorganic, Phys. Theor.* **1971**, No. 182, 182.

(26) Abraham, M. H.; Rolfe, P. H. Organometallic Compounds 4*. The Consitution of the Ethylzinc Halides. *J. Organomet. Chem* **1967**, *7*, 35–43.

(27) Koszinowski, K.; Böhrer, P. Aggregation and Reactivity of Organozincate Anions Probed by Electrospray Mass Spectrometry. *Organometallics* **2009**, *28*, 100–110.

(28) Fleckenstein, J. E.; Koszinowski, K. Lithium Organozincate Complexes LiRZnX2: Common Species in Organozinc Chemistry. *Organometallics* **2011**, *30*, 5018–5026.

(29) Hunter, H. N.; Hadei, N.; Blagojevic, V.; Patschinski, P.; Achonduh, G. T.; Avola, S.; Bohme, D. K.; Organ, M. G. Identification of a Higher-Order Organozincate Intermediate Involved in Negishi Cross-Coupling Reactions by Mass Spectrometry and NMR Spectroscopy. *Chem. Eur. J.* **2011**, *17*, 7845–7851.

(30) Stevenson, P. J. Second-Order NMR Spectra at High Field of Common Organic Functional Groups. *Org. Biomol. Chem.* **2011**, *9*, 2078.

(31) Wynn, D. A.; Roth, M. M.; Pollard, B. D. The Solubility of Alkali-Metal Fluorides in Non-Aqueous Solvents with and without Crown Ethers, as Determined by Flame Emission Spectrometry. *Talanta* **1984**, *31*, 1036–1040.

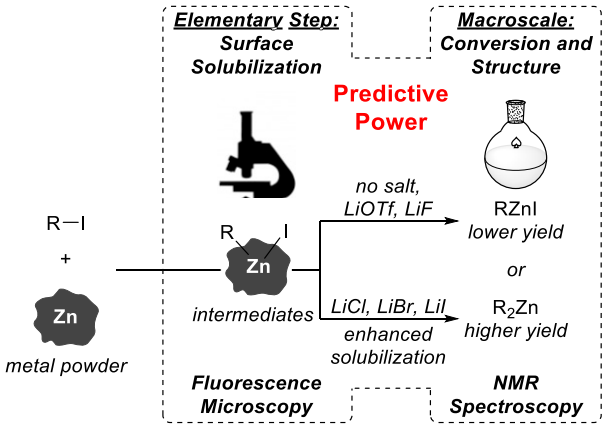
Elementary Step:
Surface Solubilization
Macroscale:
Conversion and Structure
Predictive Power
R—I
+
Zn
metal powder
R I
Zn
intermediates
no salt, LiOTf, LiF
RZnI
lower yield
or
LiCl, LiBr, LiI
enhanced solubilization
R2Zn
higher yield
Fluorescence Microscopy
NMR Spectroscopy